Scientific Reports

https://doi.org/10.1038/s41598-026-56414-8

Article in Press

Cold plasma, Fe and Mn nanoparticles modulate antioxidant activity, cannabinoids gene expression, and fatty acid profile in salt-stressed hemp

Received: 5 November 2025

Accepted: 31 May 2026

Published online: 02 June 2026

Cite this article as: Ghasempour S., Jahromi M.G., Mousavi A. *et al.* Cold plasma, Fe and Mn nanoparticles modulate antioxidant activity, cannabinoids gene expression, and fatty acid profile in salt-stressed hemp. *Sci Rep* (2026). https://doi.org/10.1038/s41598-026-56414-8

Samaneh Ghasempour, Marzieh Ghanbari Jahromi, Amir Mousavi & Alireza Iranbakhsh

Cold plasma, Fe and Mn nanoparticles modulate antioxidant activity, cannabinoids gene expression, and fatty acid profile in salt-stressed hemp

Samaneh Ghasempour[1] ▯ Marzieh Ghanbari Jahromi[2]* ▯ Amir Mousavi[3] ▯ Alireza Iranbakhsh[4]

[1] Ph.D. student, Department of Horticultural Science, SR.C., Islamic Azad University, Tehran, Iran.

[2] Assistant Professor, Department of Horticultural Science, SR.C., Islamic Azad University, Tehran, Iran.

[3] Associate Professor, Department of Plant Molecular Biotechnology, National Institute of Genetic Engineering and Biotechnology (NIGEB), Tehran, Iran.

[4] Professor, Department of Biology, SR.C., Islamic Azad University, Tehran, Iran

*Corresponding authors: *Corresponding authors: *ghanbari@iau.ac.ir*

Marzieh Ghanbari Jahromi https://orcid.org/0000-0001-9931-949X

Cold plasma, Fe and Mn nanoparticles modulate antioxidant activity, cannabinoids gene expression, and fatty acid profile in salt-stressed hemp

Abstract

Soil salinity threatens global agriculture, yet sustainable strategies for high-value crops like hemp (*Cannabis sativa* L.) remain underexplored. While seed priming with physical and nano-technologies offers promise, their potential

to enhance hemp's resilience under salt stress is unknown. This study investigates the comparative efficacy of cold plasma (CP; 60 and 90s) and metal nanoparticles (Fe NPs and Mn NPs; 50 mgL^{-1}) seed priming to mitigate salinity stress in hemp (0, 60, and 120 mM NaCl). Severe salinity (120 mM) compromised non-primed plants, reducing shoot fresh weight (39%), root fresh weight (17%), and cannabinoids; cannabidiol (CBD; 22%) and tetrahydrocannabinol (THC; 20%). Crucially, specific priming agents counteracted this stress and enhanced performance. Fe NP priming under moderate salinity (60 mM) was most effective, triggering upregulation of biosynthetic genes—*CBDAS* and *THCAS* expression increased by 102% and 170% relative to stressed controls—leading to improved cannabinoid levels and fatty acid profiles. The 90s CP treatment similarly bolstered salt tolerance. This work provides the first evidence that Fe NPs and 90s CP are effective priming strategies modulating antioxidant activity, gene expression, and lipid metabolism. These findings offer a novel approach to sustainably enhance resilience and pharmaceutical value of industrial hemp cultivated on salinized lands.

Keywords Antioxidant potential**,** Linoleic acid**,** Low-Temperature Plasma, Nano-priming**,** Salinity tolerance**,** Tetrahydrocannabinol

Introduction

Soil salinity is a growing global environmental issue that severely restricts agricultural productivity across arid and semi-arid regions. The primary

mechanisms of salinity damage include ionic toxicity (excessive Na^+ and Cl^-), osmotic stress, and the generation of reactive oxygen species (ROS), which collectively impair plant growth, nutrient uptake, and metabolic function [1, 2]. Climate change induced reductions in streamflow and increased drought frequency, as projected by machine learning models, can limit freshwater for irrigation and thereby exacerbate soil salinization [3]. Among emerging approaches, cold plasma (CP) seed priming and nanoparticle (NP) applications have shown promise in enhancing plant stress resilience through physical and nanotechnological interventions.

Despite the promise of these strategies, the underlying ionic imbalance caused by salinity significantly threatens cannabinoid metabolism in industrial hemp (*Cannabis sativa* L.) by disturbing the balance of ions and hindering the absorption of vital nutrients. High sodium levels especially reduce magnesium availability, which is a crucial cofactor for enzymes involved in cannabinoid production [4, 5]. This environmental stress also causes oxidative damage by generating ROS, triggering antioxidant responses that affect both the quantity and composition of cannabinoids [6, 7]. Additionally, salinity leads to changes in gene expression, potentially altering the metabolic pathways responsible for cannabinoid synthesis [8]. Understanding these physiological changes is essential for improving farming practices and developing strategies to maintain cannabinoid yields in crops grown in saline soils [9].

Cold plasma (CP) seed priming is a novel physical method that operates through multiple interconnected mechanisms. The partially ionized gas generates reactive oxygen and nitrogen species (RONS), which upon seed imbibition trigger mild oxidative stress, activating signal transduction cascades such as those involving hydrogen peroxide (H_2O_2) and nitric oxide (NO) as secondary messengers [10]. This preconditioning enhances the expression of genes encoding antioxidant enzymes (e.g., superoxide dismutase (SOD), catalase (CAT), ascorbate peroxidase), thereby strengthening the cellular redox defense system [11]. Additionally, CP treatment modifies seed coat permeability, facilitating improved water uptake and ion homeostasis under salinity. It also upregulates genes involved in ion transport (e.g., HKT, NHX) and osmotic adjustment (e.g., proline biosynthesis), collectively maintaining cellular turgor and reducing Na^+ accumulation [11]. These mechanisms have been documented in various crops; for example, in tomato (*Solanum lycopersicum*) and rice (*Oryza sativa*), CP priming consistently improved germination, biomass, and photosynthetic efficiency under saline conditions, as well as enhanced the accumulation of valuable secondary metabolites [10, 12].

Nanoparticle applications offer complementary and mechanistically distinct approaches for salinity stress mitigation [13]. Iron nanoparticles (Fe NPs) primarily act as slow-release sources of Fe^{2+}/Fe^{3+}, a critical cofactor for chlorophyll synthesis, electron transport chain components, and ROS-scavenging enzymes such as CAT and peroxidase. By optimizing ionic balance

and reducing oxidative burst, Fe NPs preserve chloroplast ultrastructure and sustain photosynthetic carbon assimilation [14]. Extensive reports have confirmed the role of Fe NPs in salt tolerance; for instance, in wheat, Fe NPs improved K^+/Na^+ ratio and enhanced antioxidant defense under saline conditions [15]. Manganese nanoparticles (Mn NPs) facilitate osmotic adjustment by stimulating the accumulation of compatible solutes including proline, glycine betaine, and soluble sugars, which stabilize membrane integrity and protect protein function under dehydration stress [16, 17]. Furthermore, Mn NPs upregulate the expression of aquaporin genes (e.g., PIPs, TIPs), enhancing root hydraulic conductance and whole-plant water use efficiency, thereby alleviating salinity-induced water deficit [18]. Studies in rice and pepper show that Mn NPs priming reduces Na^+ uptake and improves germination under salinity [19, 20], while insights from *Arabidopsis* and maize confirm its role in enhancing antioxidant defense and root growth [21, 22].

While industrial hemp (*Cannabis sativa* L.) is generally considered a plant that can grow in low salinity soils [23], this tolerance is not absolute. It can withstand low to moderate salinity levels, approximately 60–80 mM NaCl, without severe growth reduction [23, 24]. However, higher concentrations (≥120 mM NaCl) have been shown to significantly compromise both biomass production and the biosynthesis of valuable secondary metabolites, including cannabinoids [25]. Therefore, even in a relatively tolerant species, priming strategies that further enhance salinity resilience are economically relevant.

The plant produces cannabinoids notably cannabidiol (CBD) and Δ^9-tetrahydrocannabinol (THC) alongside terpenoids and flavonoids with demonstrated therapeutic potential [26]. CBD exhibits diverse pharmacological properties, including anti-inflammatory, analgesic, and neuroprotective activities, supporting its investigation for various medical applications [27]. THC, the primary psychoactive constituent, constitutes the active component in nabiximols, an approved botanical medication for managing multiple sclerosis symptoms [28]. The biosynthetic pathway of cannabinoids involves key enzymes such as cannabidiolic acid synthase (CBDAS) and tetrahydrocannabinolic acid synthase (THCAS), which convert the common precursor cannabigerolic acid (CBGA) into CBDA and THCA, respectively. The expression levels of the corresponding genes, *CBDAS* and *THCAS*, directly determine the final CBD and THC content in hemp tissues [29]. Understanding how abiotic stresses and priming treatments affect these genes is therefore crucial for optimizing cannabinoid yields.

Research on CP and NP applications for salinity mitigation in hemp is still emerging. Ivankov et al. (2020) applied a 2-min CP treatment to hemp seeds [30]. Although germination improved in vitro, no significant effect was observed in the field; moreover, CP caused a 41% reduction in leaf CBDA content, indicating potential adverse effects on cannabinoid quality. Their study did not include salinity stress. Iranbakhsh et al. (2020) used a 40-s CP treatment under *in vitro* conditions and reported enhanced antioxidant activity together with upregulation of cannabinoid biosynthesis genes at the

seedling stage (plants ~10 cm tall); however, their study also lacked salinity stress [31]. Most recently, Ghasempour et al. (2024) showed improved germination, water relations, and antioxidant metabolism in hemp under salt stress following CP and NP priming [25]. While these studies provide valuable preliminary evidence, critical knowledge gaps persist: no systematic comparative assessment of CP versus Fe NPs versus Mn NPs has been conducted in hemp under moderate to severe salinity, and the effects on cannabinoid profiles, their biosynthetic gene expression (*CBDAS*, *THCAS*), and fatty acid composition remain unexplored. Therefore, this study fills this gap by providing the first comparative assessment of Fe NPs, Mn NPs, and CP as separate seed priming treatments under salinity stress in hemp, integrating analyses of biomass, antioxidant enzymes, cannabinoids, gene expression, and fatty acid profiles.

To better contextualize our approach, it is useful to compare chemical and biophysical priming strategies. Chemical priming relies on exogenous application of compounds such as hydrogen peroxide, salicylic acid, or halo-agents (e.g., $CaCl_2$, KCl) to induce stress memory and activate defense pathways [32]. While effective, chemical priming often faces limitations including potential phytotoxicity at high concentrations, environmental persistence, and inconsistent results across species and growth stages [33]. In contrast, biophysical priming methods such as CP treatment offer a residue-free, environmentally friendly alternative with rapid application and no chemical accumulation in plant tissues [34]. Similarly, NP priming

provides targeted nutrient delivery and sustained release, reducing the risk of toxicity compared to bulk chemical salts [14]. However, biophysical methods may require specialized equipment and optimization of exposure parameters. Both strategies share the common goal of enhancing stress resilience, and their comparative evaluation under identical conditions remains limited, particularly in hemp.

A key conceptual framework underlying this research is that both CP and NPs function as effective elicitors of secondary metabolism in plants. Elicitors are agents that trigger defense responses and stimulate the biosynthesis of specialized metabolites, including cannabinoids, terpenoids, and phenolics. In medicinal plants, abiotic elicitors such as NP and physical stresses have been shown to upregulate key biosynthetic genes and enhance the accumulation of pharmaceutically valuable compounds [35, 25]. Therefore, beyond their role in stress mitigation, CP and NP priming may directly influence cannabinoid biosynthesis, offering a dual benefit: alleviating salt-induced damage while simultaneously improving the quality and quantity of hemp's therapeutic metabolites.

Given the economic importance of hemp for pharmaceutical applications and the identified knowledge gaps, we selected this plant as our model. The overarching aim of this study is to elucidate the comparative effects of seed priming with CP, Fe NPs, and Mn NPs on the physiological, biochemical, and molecular responses of hemp under moderate (60 mM) and severe (120 mM) salinity stress. We hypothesize that (1) each priming treatment will alleviate

salinity-induced oxidative damage and improve growth performance; (2) Fe NPs and Mn NPs will enhance salt tolerance through distinct mechanisms related to nutrient homeostasis and osmotic adjustment; (3) CP priming will upregulate antioxidant defense genes and ion transporters; and (4) all three priming agents will act as elicitors of secondary metabolism, increasing the expression of *CBDAS* and *THCAS* and subsequently enhancing cannabinoid content and fatty acid profiles, with Fe NPs showing the most pronounced effect under moderate salinity. This investigation therefore examines how CP, Fe NPs, and Mn NPs seed priming modulates shoot-root biomass, antioxidant defenses, cannabinoid composition, associated gene expression, and fatty acid profiles in salinity-stressed hemp. Our findings aim to establish scientific foundations for practical interventions that sustain crop productivity and pharmaceutical quality in salt-affected agricultural systems.

Materials and Methods

Growth conditions

A factorial experiment was arranged in a completely randomized design with three replications under greenhouse conditions in 2024. Each biological replicate consisted of two plastic pots (3 L each), and each pot contained two plants. Initially, four seeds were sown per pot; after germination and prior to the flowering stage, male plants (if any) were removed, leaving two uniform female plants per pot. Thus, each replicate comprised four plants. Each pot was considered an experimental unit, and pots were randomly arranged on greenhouse benches. Day and night temperatures averaged 28 °C and 14 °C,

respectively, with relative humidity maintained at 65 to 75%. Certified hemp seeds, sourced from Pakanbazr Co., were surface-sterilized and cultivated in 3-L plastic pots filled with loamy soil (pH 7.2; EC 1.2 dS m^{-1}). The first experimental factor consisted of five seed priming treatments; CP-60s (cold plasma at 60 seconds), CP-90s (cold plasma at 90 seconds), Fe NPs (iron nanoparticles), Mn NPs (manganese nanoparticles), and an unprimed control. The concentrations of Fe and Mn NPs (50 mg L^{-1}) were selected based on previous reports showing that 50 mg L^{-1} Fe NPs effectively improved salt tolerance in hemp [25]. For CP exposure, a preliminary experiment tested durations from 40 to 120 s; based on seedling growth and stress tolerance, the range of 60–100 s was found optimal. Therefore, 60 and 90 s were chosen as representative treatments. Salinity levels of 0, 60, and 120 mM NaCl were selected to represent non-stress, moderate, and severe stress, respectively, as supported by literature [36, 25]. For the NP treatments, seeds were immersed in 50 mg L^{-1} suspensions of Fe NPs or Mn NPs for 6 hours; for the CP treatments, seeds were exposed to the plasma source for the designated time as detailed below. The total number of pots was five priming treatments × 3 salinity levels × 3 replicates × 2 pots per replicate = 90 pots. After male removal, each pot contained 2 uniform female plants (total 180 plants).

Salinity stress was initiated at the six-leaf stage (approximately six weeks after sowing). NaCl solutions (0, 60, and 120 mM) were applied via gentle irrigation around the base of each plant at a volume of 300 mL per pot every three days for a total of 40 days. Each pot was placed on an individual saucer

to collect any drainage water. To prevent waterlogging and reabsorption of leached salts, the saucers were emptied within 30 minutes after each irrigation and the drainage water was discarded. Pots were spaced sufficiently apart to prevent cross-contamination. All pots within each salinity level received the same volume of NaCl solution, and the application was carried out consistently throughout the 40-day period.

To monitor the actual salinity exposure of the plants, the electrical conductivity (EC) of the collected drainage water was measured weekly for each pot using a portable EC meter (model TES-1381, TES Electrical Electronic Corp., Taiwan). The EC of the applied NaCl solutions (0, 60, and 120 mM) was also measured at the same frequency as a reference. This approach allowed us to verify that the salt concentration to which the plants were exposed remained consistent throughout the experiment and to detect any drift due to evaporation or salt accumulation.

Cold plasma characteristics

The cold plasma system utilized a high-voltage AC power supply operating at 11 kV and 23 kHz. The configuration incorporated parallel glass plates serving as dielectric barriers between copper electrodes, with argon as the carrier gas at a flow rate of 3 L min^{-1}. The distance between the upper electrode and the seed surface was fixed at 8 mm. Input power was set to 250 W, and the power density, estimated as input power divided by the electrode area (78 cm^2), was 3.2 W cm^{-2}. Seeds were placed in a single layer without agitation during exposure. Seed surface temperature was monitored before

and immediately after treatment using an infrared thermometer; the temperature increases never exceeded 5 °C above room temperature (maximum measured 32 °C). Microdischarges formed when the interelectrode potential reached the breakdown threshold of the dielectric material, following established principles [37].

Nanoparticle Characterization

The Fe_2O_3 (alpha) and Mn_2O_3 nanoparticles used in this study were purchased from Pishgaman Nano Materials Iranian Co. (Tehran, Iran), which supplied US-Nano (USA) products (catalog No. US3180 and US3340). According to the manufacturer's specifications: Fe_2O_3 nanoparticles had an average particle size of 30 nm, purity ≥ 99.5%, spherical morphology, true density 5.24 g cm^{-3}, and specific surface area 20–60 m^2 g^{-1}. Mn_2O_3 nanoparticles had an average size of 30 nm, purity ≥ 99.2%, spherical morphology, bulk density 0.35 g cm^{-3}, and specific surface area 150 m^2 g^{-1}. For dispersion, nanoparticles were suspended in deionized water (pH ~ 7.0, unadjusted) and sonicated (40 kHz, 100 W, 30 min) immediately before use; no stabilizers or surfactants were added. The dispersion was used without filtration, and sterility was ensured by working under a laminar flow hood. To distinguish nanoparticle-specific effects from ionic toxicity, additional ionic control treatments were included: $FeCl_2$ (50 mg L^{-1} Fe^{2+}) and $MnCl_2$ (50 mg L^{-1} Mn^{2+}). The ionic controls consistently showed lower protective effects than the nanoparticles, confirming that the observed benefits are attributable to the nano-form of the elements.

Plant biomass measurement

At physiological maturity (mid-flowering stage), representative plants were selected from each pot for biomass evaluation. Shoot and root systems were carefully separated, and fresh weights were recorded for individual plant components.

Enzymatic assays

Catalase (CAT) activity was determined according to Roosta et al. (2025) [38] by monitoring H_2O_2 decomposition at 240 nm. Leaf tissues were homogenized in 50 mM potassium phosphate buffer (pH 7.0) containing 1% polyvinylpolypyrrolidone (PVPP), 1 mM ethylenediaminetetraacetic acid (EDTA), and 1 mM phenylmethylsulfonyl fluoride (PMSF). The assay mixture consisted of 50 mM phosphate buffer (pH 7.0), 3% H_2O_2, and 0.1 mM EDTA. One enzyme unit was defined as µmol H_2O_2 decomposed per minute per mg protein.

Superoxide dismutase (SOD) activity was measured using the photochemical method described by Shams et al. (2024) [39]. The reaction solution contained 50 mM phosphate buffer (pH 7.8), 13 mM methionine, 75 µM nitroblue tetrazolium (NBT), 0.1 mM EDTA, and 2 µM riboflavin. The reaction was initiated by illuminating samples for 60 minutes at 30°C, with dark-incubated mixtures serving as blanks. SOD activity was quantified by measuring the inhibition of NBT reduction at 560 nm.

Determination of Cannabinoid Content

Cannabinoid extraction and quantification followed established chromatographic methods. Dried floral material was pulverized, and the target compounds (THC and CBD) were extracted into an organic solvent. After solvent evaporation, the residue was reconstituted for high-performance liquid chromatography (HPLC) analysis. Separation was achieved on a C18 reversed-phase column with an isocratic mobile phase of methanol and water (80:20 v/v) at a flow rate of 1 mL min^{-1}. Detection was performed with a UV-Vis detector set at 230 nm. Quantification was based on external calibration curves generated from pure THC and CBD standards. A series of standard solutions were injected, and the resulting peak areas were plotted against concentration to produce a linear calibration model (R^2 > 0.99), which was used to calculate sample concentrations [40].

RNA Extraction and cDNA Synthesis

Total RNA was isolated from tissue samples using the GenUPTM Total RNA Kit (Biotechrabbit, Germany). RNA integrity was verified via agarose gel electrophoresis, and purity was assessed with a NanoDrop spectrophotometer (Thermoscientific 2000c, USA). To eliminate genomic DNA contamination, the extracts were treated with DNase (Fermentase, USA). Subsequently, first-strand complementary DNA (cDNA) was synthesized from the purified RNA using the AddScript cDNA Synthesis Kit (Addbio, Korea, Cat No. 22701) according to the manufacturer’s protocol.

Molecular Analysis

The relative expression levels of the *THCAS* and *CBDAS* genes were quantified using quantitative real-time PCR (qRT-PCR). Gene-specific primer pairs were designed from the corresponding gene sequences using the PrimerQuest Tool (Integrated DNA Technologies). The sequences of the primers utilized in this research are listed in Table 1.

Prior to qRT-PCR, conventional endpoint PCR was performed to verify primer specificity and amplicon size. These reactions were carried out in a thermal cycler (Bio-Rad) using a mixture containing 1× PCR buffer, 0.4 µM of each forward and reverse primer, 0.2 mM deoxynucleotide triphosphates (dNTPs), 200 ng of cDNA template, and 1 unit of Taq DNA Polymerase. The thermal cycling protocol comprised an initial denaturation step at 94 °C for 5 minutes, followed by 35 cycles of denaturation, annealing, and extension. The resulting PCR products were separated by electrophoresis on a 2% agarose gel and visualized under UV light after ethidium bromide staining.

For the qRT-PCR analysis, reactions were performed on an Azure Cielo Real-Time PCR system. Each 20 µL reaction contained 8 µL of EvaGreen Master Mix, 1.5 µL of diluted cDNA, 0.25 µM of each primer, and PCR-grade water to volume. The ubiquitin (UBQ) gene was used as an endogenous reference for data normalization. Non-template controls (NTCs) were included in each run, consistently yielding Cq values at or above 40.

To assess the potential for PCR inhibition, a subset of samples was serially diluted tenfold and amplified with the UBQ primer set. The amplification efficiency for each gene target was calculated directly by the Azure Cielo

software from the standard curve generated by dilution series. Only reactions with a calculated PCR efficiency of 80% or greater (corresponding to a slope between -3.1 and -3.6) were included in the final gene expression analysis.

All experiments were conducted with a minimum of three biological replicates. Statistical analysis of relative gene expression was performed using the REST software package.

Fatty Acid Profiling

The oil extraction was conducted following a standard Soxhlet procedure with a 1:1 (v/v) chloroform/methanol solvent system [41]. For fatty acid composition analysis, the extracted oils were derivatized to their corresponding fatty acid methyl esters (FAMEs). Briefly, 0.1 g of oil was combined with 3 mL of heptane and 0.05 mL of a methanolic potassium hydroxide solution to catalyze the transesterification reaction. The generated FAMEs were subsequently analyzed using a DANI model 1000-GC gas chromatograph (GC). Separation was achieved on an HP-5MS capillary column (30 m × 0.32 mm i.d., 0.25 µm film thickness), with high-purity nitrogen as the carrier gas flowing at 1 mL min^{-1}. The injector and flame ionization detector (FID) temperatures were held constant at 250 °C and 280 °C, respectively.

Statistical Evaluation

Data were subjected to a two-way analysis of variance (ANOVA) appropriate for a factorial completely randomized design using SAS statistical software. The main factors were seed priming (5 levels) and salinity stress (3 levels),

and their interaction was included in the model. Mean comparisons were performed only when the interaction effect was significant ($p \leq 0.05$) using the Least Significant Difference (LSD) test at $\alpha = 0.05$. Furthermore, data relationships were visualized through a heat map constructed with CIMminer, an online application for clustering and graphical representation of multidimensional data.

Results

Biomass Accumulation in Shoot and Root Tissues

Exposure to salinity stress led to a significant reduction in plant biomass. In contrast, seed priming with CP, iron nanoparticles (Fe NPs), and manganese nanoparticles (Mn NPs) effectively counteracted this negative effect. Under non-primed plants, a salinity level of 120 mM caused a pronounced decrease in shoot and root dry weight by 39% (Figure 1a) and 17% (Figure 1b), respectively, relative to the non-stressed control. The application of priming agents, however, markedly improved biomass production under salt stress. Specifically, in plants subjected to 120 mM salinity, priming with CP for 60 s, CP for 90 s, Fe NPs, and Mn NPs enhanced shoot biomass by 22%, 27%, 37%, and 30%, respectively, compared to the non-primed plants, salt-stressed group (Figure 1a). A similar promotive effect was observed in root tissues, with corresponding increases of 10%, 13%, 19%, and 16% (Figure 1b).

Activity of Antioxidant Enzymes

The enzymatic antioxidant system was significantly modulated by salinity stress. In the absence of seed priming, the 120 mM salinity treatment induced

a substantial upsurge in the activity of SOD and CAT by 95% (Figure 2a) and 83% (Figure 2b), respectively, compared to the control plants. The priming treatments also elevated the activity of these enzymes, though to a lesser extent than the severe salt stress. For instance, under a moderate salinity level of 60 mM, seed pretreatment with CP 60 s, CP 90 s, Fe NPs, and Mn NPs resulted in SOD activity increases of 22%, 17%, 22%, and 6%, respectively (Figure 2a). A comparable trend was recorded for CAT activity, which was augmented by 10%, 26%, 25%, and 26% under the same conditions (Figure 2b).

Cannabinoids

The results indicated that under moderate salinity conditions, there was an increase in the cannabinoids. However, when the salinity stress level was intensified to 120 mM, the opposite trend was observed, with a significant decrease in both CBD and THC concentrations in the plants that were not subjected to seed priming. Under moderate salinity conditions, there was a relative increase in CBD (Figure 3a) and THC (Figure 3b) levels. When salinity reached 120 mM, CBD decreased by 22% and THC decreased by 25% compared to the control without seed priming. In plants exposed to salinity at 120 mM, seed priming with CP 60 s, CP 90 s, Fe NPs, and Mn NPs resulted in enhancements of CBD by 20, 23, 26, and 22%, respectively, relative to the control (Figure 3a). These treatments also increased THC levels by 18, 22, 23, and 25%, respectively (Figure 3b).

Gene expression of cannabinoids

THCAS and *CBDAS* expression significantly increased under salinity at 60 mM, but decreased at 120 mM. Seed priming with CP, Fe NPs, and Mn NPs significantly boosted the expression of these genes. In non-primed plants, salinity at 60 mM dramatically boosted *CBDAS* and *THCAS* expression by 80% (Figure 4a) and 140% (Figure 4b), respectively. On the other hand, the addition of salt decreased *THCAS* and *CBDAS* expression by 35 and 34%, respectively. Moreover, seed priming with CP, Fe NPs, and Mn NPs enhanced the expression of *THCAS* and *CBDAS*. For example, compared to the control, the expression of *THCAS* and *CBDAS* rose by 162% and 119%, respectively, after applying 60 mM of salinity and 90 s of CP.

Fatty acid profile

Salinity increased the content of palmitic acid (C16:0), whereas seed priming with CP, Fe NPs, and Mn NPs showed a decreasing trend. Under non-primed plants, salinity at 60 and 120 mM increased palmitic acid levels by 12% and 15%, respectively, compared to non-stressed treatments. However, stearic acid (C18:0) did not show significant changes across treatments. Its highest level was observed under 60 mM salinity and Mn NP treatment, with an 18% increase relative to the control. Oleic acid (C18:1) decreased under salinity stress but increased following seed priming with CP, Fe NPs, and Mn NPs. Salinity at 120 mM reduced oleic acid content by 13% compared to the control in non-primed plants. In contrast, linoleic acid (C18:2) increased under salinity, with the highest level recorded under non-primed plants with 120 mM salinity, showing a 10% increase relative to the control. However,

seed priming with CP, Fe NPs, and Mn NPs led to a decrease in linoleic acid content. Linolenic acid (C18:3) decreased under salinity, with a 19% reduction observed at 120 mM salinity. In contrast, seed-primed plants exhibited higher levels of linolenic acid. Specifically, CP 60 s, CP 90 s, Fe NPs, and Mn NPs increased linolenic acid content by 11%, 18%, 22%, and 23%, respectively, compared to the control (Table 2).

The hierarchical clustered heatmap

The hierarchical clustered heatmap (Figure 5) was generated using row-wise Z-score normalization, which scales each variable (antioxidant enzyme, cannabinoid, gene expression, fatty acid, growth parameter) to zero mean and unit variance. This method highlights relative treatment-specific patterns rather than absolute values.

Under salinity stress (Figure 5a), increasing salinity from 0 to 120 mM NaCl progressively increased the relative intensity of CAT and SOD. The relative levels of THC, CBD, and the expression of *THCAS* and *CBDAS* genes were highest at 60 mM NaCl. Growth parameters (shoot and root weight) showed a decreasing relative intensity with higher salinity. For the fatty acid profile, palmitic, stearic, oleic, linoleic, and linolenic acids exhibited distinct color changes across salinity levels, with no single pattern of stability.

In the second heatmap (priming treatments, Figure 5b), cold plasma (CP 60 s, CP 90 s), iron (Fe NPs), and manganese (Mn NPs) treatments were compared against the control. CP (90 s) and Fe NPs treatments showed increased relative intensities for CBD, THC, SOD, and CAT compared to the

control. Mn NPs treatment showed relatively higher intensities for oleic and palmitic acids. Trait clustering revealed associations among cannabinoids and antioxidants, while treatment clustering separated CP 90 s and Fe NPs from the control and Mn NPs groups.

Discussion

Our results demonstrated that seed priming with CP and metal NPs (Fe NPs and Mn NPs) significantly alleviated salinity-induced growth reduction in hemp, with Fe NPs and 90 s CP showing the strongest protective effects (Figures 1-4). Salinity stress is a major abiotic constraint that significantly impairs hemp growth, primarily through a substantial reduction in biomass accumulation. Elevated salt concentrations disrupt key physiological functions by inducing osmotic stress, limiting water availability, and impairing photosynthetic efficiency. The accumulation of sodium and chloride ions in plant tissues further aggravates these effects by inducing nutrient imbalances and metabolic dysfunction. Subsequent oxidative stress, triggered by reactive oxygen species (ROS) overproduction, inflicts damage to cellular structures including membranes, proteins, and nucleic acids, ultimately compromising plant viability [9]. Although plants activate antioxidant systems as a countermeasure, sustained stress exposure can overwhelm these protective mechanisms, leading to progressive growth deterioration [42].

In recent years, various priming strategies have been developed to enhance plant stress tolerance. Among them, chemical priming—using compounds

such as hydrogen peroxide, salicylic acid, or halo-agents—can induce stress memory and activate defence pathways [32]; however, its practical application is often limited by potential phytotoxicity at higher concentrations, environmental persistence of residues, and inconsistent results across different species [33]. Biophysical priming approaches, including CP and NP treatments, offer attractive alternatives. CP treatment is residue-free, rapid, and leaves no chemical accumulation in plant tissues [34], while NP priming provides targeted nutrient delivery and sustained release, thereby reducing the toxicity risk associated with bulk chemical salts [14]. Importantly, the beneficial effect of 50 mg L^{-1} NPs in our study follows a hormetic response, similar to Zn/ZnO NPs in tomato and wheat [48]. NP effects are highly dependent on concentration, particle size, agglomeration state, and exposure conditions; higher concentrations or less stable formulations could induce oxidative stress or nutrient imbalance [48]. In the present study, the chosen concentration (50 mg L^{-1}) did not cause visible phytotoxicity – although subtle adverse effects cannot be entirely excluded – and both CP and NP priming effectively improved hemp performance under salinity, with Fe NPs and 90 s CP showing the strongest effects across multiple measured traits (Figures 1-4).

Cold plasma (CP) seed priming emerges as a promising strategy to mitigate salinity impacts. This treatment enhances germination performance, seedling establishment, and subsequent growth through multiple interconnected mechanisms. Beyond the direct effects of UV photons and charged particles,

CP generates reactive oxygen and nitrogen species (RONS) that act as signaling molecules, modifies seed coat permeability (increasing wettability), and improves water uptake and ion homeostasis under salinity [10, 11]. Under saline conditions, CP application improves plant weight through multiple mechanisms: enhanced water-use efficiency reduces dehydration risks, optimized nutrient assimilation counteracts salinity-induced deficiencies, and increased photosynthetic capacity promotes biomass accumulation [43]. Specifically, in our study, CP priming for 90 s increased shoot biomass by 27% and root biomass by 13% under 120 mM NaCl compared to non-primed stressed plants (Figure 1). These results are consistent with Shirkhani et al. (2025) [42], who reported that CP treatment (60-120 s) enhanced shoot and root biomass in summer savory under 100 mM NaCl. Thus, a 90 s CP exposure is particularly effective for hemp under severe salinity.

In our experiment, Fe NP priming (50 mg L^{-1}) increased shoot and root biomass by 37% and 19%, respectively, under 120 mM NaCl (Figure 1). This is comparable to findings in wheat, where 50 mg L^{-1} Fe NPs improved K^+/Na^+ ratio and enhanced antioxidant defense under 100 mM NaCl [15]. Similarly, Mn NP priming (50 mg L^{-1}) in our study increased shoot biomass by 30% under severe salinity, which aligns with reports in rice and pepper where Mn NPs (50-100 mg L^{-1}) reduced Na^+ uptake and improved germination under high salinity [19, 20].

The regulatory effects on antioxidant enzymes constitute a key mechanism shared by both salinity stress and priming treatments. Salt-induced ROS generation, including superoxide radicals and hydrogen peroxide, necessitates activation of enzymatic antioxidants like SOD and CAT to maintain cellular redox homeostasis [44]. Seed priming with CP and metal NPs potentiates this native defense system. Increased antioxidant enzyme activity can reflect higher oxidative stress rather than improved resistance. However, in the present study the observed increases in SOD and CAT were accompanied by improved growth parameters and reduced visual symptoms of oxidative stress in primed plants. Therefore, we interpret the enzyme upregulation as a beneficial preconditioning response that helps maintain redox balance under salinity, though a direct causal link to stress alleviation should be drawn cautiously. In our study, under 60 mM NaCl, SOD activity increased by 22% with Fe NP priming and by 17% with 90 s CP priming (Figure 2a). CAT activity increased by 25% with Fe NPs and 26% with Mn NPs under the same conditions (Figure 2b). These observations are consistent with previous reports: in tomato, Adhikari et al. (2020) [10] found that CP priming (60-90 s) up-regulated SOD and CAT gene expression under salt stress; in wheat, Fe NPs (50 mg L^{-1}) enhanced CAT and peroxidase activities under 100 mM NaCl [15]. Seed priming with CP, Fe NPs, and Mn NPs improved the activity of SOD and CAT by triggering a mild oxidative stimulus. The CP-generated RONS (including H_2O_2 and NO) and modified seed surface properties (increased wettability, altered coat permeability)

collectively pre-activate antioxidant systems, making plants more resilient [42, 10]. Furthermore, the presence of Fe and Mn NPs improves their bioavailability and uptake, supporting enzymatic structure and function. This priming effect leads to a more robust antioxidant system that responds more effectively to salinity-induced oxidative stress, maintaining redox balance, reducing cellular damage, and supporting plant growth and stress resilience; this was manifested in the present study as improved overall plant health and biomass production of hemp plants under salt stress (Figure 6).

Salinity stress differentially regulates cannabinoid biosynthesis, with the effect being highly dependent on its severity. Under moderate salinity stress, hemp plants activate stress responses, such as the mitogen-activated protein kinase (MAPK) cascade and calcium-mediated signaling pathways. Stress-responsive transcription factors are upregulated, triggering the expression of genes involved in secondary metabolite biosynthesis, including cannabinoids [27]. In this moderate stress regime, ROS can act as signaling molecules that activate antioxidant enzymes and induce the expression of genes encoding enzymes in cannabinoid biosynthesis pathways, potentially leading to higher CBD concentrations as reported by Formisano et al. (2024) [27] at salinity levels of 4 to 6 dS m^{-1}. Conversely, severe salinity stress disrupts essential physiological processes in hemp plants, causing pronounced osmotic stress, ion toxicity, and reduced photosynthetic efficiency. This severe disruption compromises carbon assimilation and diverts resources away from secondary metabolism, ultimately

downregulating cannabinoid biosynthesis pathways and resulting in lower levels of CBD and THC. Our data support this biphasic response: under 60 mM NaCl, CBD and THC levels increased relative to control, while under 120 mM NaCl they decreased by 22% and 25%, respectively, in non-primed plants (Figure 3).

Seed priming with CP, Fe NPs, and Mn NPs can enhance the expression of genes related to CBD and THC biosynthesis in *Cannabis sativa* plants. In our study, under 60 mM NaCl and 90 s CP priming, *CBDAS* expression increased by 119% and *THCAS* expression by 162% compared to the non-stressed control (Figure 4). Under the same salinity level, Fe NP priming increased *CBDAS* by 102% and *THCAS* by 170% (Figure 4). The magnitude and direction of gene expression changes varied with treatment and salinity level. For instance, under 120 mM NaCl, all priming treatments increased *CBDAS*/*THCAS* expression compared to the non-primed stressed control, but the absolute transcript levels remained lower than those observed under 60 mM NaCl. This indicates that the priming effect is salinity-dependent and likely involves different regulatory mechanisms under moderate versus severe stress. These treatments act as beneficial priming stimuli that trigger mild oxidative stress, activating stress response genes, modulating ROS signaling, and influencing metabolic pathways. CP can up-regulate genes involved in cannabinoid biosynthesis, trigger antioxidant defense mechanisms, and promote secondary metabolite accumulation, as demonstrated by Iranbakhsh et al. (2020) [31], who found that CP (40-80 s)

up-regulated *CBDAS* and *THCAS* expression by 12-25 fold. Fe NPs can serve as biocompatible carriers, modulate membrane permeability, and enhance the activity of enzymes related to cannabinoid biosynthesis. Similarly, Mn NPs (50 mg L^{-1}) in our study increased *CBDAS* and *THCAS* expression by approximately 80-100% under 60 mM NaCl (Figure 4), which is consistent with the work of Ye et al. (2020) [20] showing that Mn NPs up-regulate stress-related genes in pepper. While our data show a positive association between increased *CBDAS*/*THCAS* transcript levels and higher CBD/THC concentrations under priming treatments, this relationship should be interpreted as an association rather than a direct causal link, because cannabinoid accumulation is also limited by precursor availability (e.g., CBGA), enzyme activity regulation, and post-transcriptional factors, none of which were measured here. Thus, additional experiments are needed to confirm whether the observed transcriptional upregulation directly drives metabolite increases.

The main changes in fatty acid profile were related to salinity. Under salinity stress, plants increase the proportion of saturated fatty acids (SFAs) like palmitic acid in their membrane lipids as a protective strategy, because they pack more tightly in the lipid bilayer, reducing fluidity, stabilizing the membrane structure, preventing ion leakage, and maintaining membrane integrity [37]. In our study, under 120 mM NaCl, palmitic acid (C16:0) increased by 15% in non-primed plants compared to the control (Table 2). Salinity stress induced a notable elevation in linoleic acid content, a key

polyunsaturated fatty acid (PUFA) constituent of hemp. Specifically, we observed a 10% increase in linoleic acid (C18:2) under 120 mM NaCl in non-primed plants (Table 2). This increase is physiologically significant, as PUFAs contribute to the preservation of membrane fluidity under osmotic stress, thereby facilitating the proper functioning of integral membrane proteins and transporters. Furthermore, PUFAs act as biosynthetic precursors for lipid-derived signaling molecules, including jasmonic acid, which are pivotal in orchestrating adaptive responses to environmental challenges [45]. This pattern of PUFA accumulation, coupled with a concurrent decline in monounsaturated fatty acids (MUFAs), aligns with observations in *Physalis alkekengi* L. subjected to saline conditions [46]. In our experiment, oleic acid (C18:1, a MUFA) decreased by 13% under 120 mM NaCl in non-primed plants (Table 2). The reduction in MUFAs suggests a strategic rechanneling of resources, wherein these compounds may be utilized as substrates for the synthesis of more highly unsaturated fatty acids via desaturase-mediated pathways, reflecting a dynamic metabolic reprogramming [47]. Conversely, seed priming with CP and mineral NPs counteracted the stress-induced fatty acid profile. For example, Fe NP priming under 120 mM NaCl reduced palmitic acid by approximately 8% and increased oleic acid by 12% compared to non-primed stressed plants (Table 2). Similarly, 90 s CP priming increased linolenic acid (C18:3) by 18% under severe salinity (Table 2). These treatments effectively attenuated the salinity stress, leading to a metabolic shift characterized by a reduction in saturated

fatty acids (SFAs) and a promotion of MUFAs [37]. This restoration of lipid homeostasis is consistent with the concurrent enhancement of antioxidant capacity and photosynthetic efficiency reported in primed plants. By mitigating oxidative damage and improving energy status, these treatments reduce the necessity for drastic membrane lipid remodeling, ultimately resulting in improved membrane integrity and function under duress [47].

Our heatmap clustering (Figure 5b) showed that CP and Fe NP treatments formed a distinct cluster from the control. Similarly, in laser-primed sage, heatmap clustering distinctly separated biophysical priming from control, reflecting treatment-specific metabolic profiles [49].

Conclusions

This study highlights the promise of cold plasma and metallic nanoparticles as innovative seed priming techniques to mitigate salt stress in hemp under controlled greenhouse conditions – a system widely used by commercial hemp growers and a relevant precursor for field applications. The results demonstrate that these priming methods can activate protective mechanisms, modulate gene expression related to cannabinoid biosynthesis, and improve the nutritional quality of hemp through modifications in the fatty acid profile. Given that the experiments were conducted with a single genotype and limited environmental conditions, further validation under field conditions and multi-location trials is necessary before broad agricultural recommendations can be made. Additionally, long-term safety assessments (particularly for nanoparticle use) and dose optimization are recommended.

Nevertheless, the present findings provide a strong basis for pilot-scale testing both in greenhouses and in the field, with hemp serving as a model for other high-value crops under saline stress.

Funding not applicable.

Acknowledgements Not applicable.

Author Contribution Samaneh Ghasempour conducted the experiments, collected the data, performed the statistical analysis, and contributed to the writing and revision of the manuscript. Marzieh Ghanbari Jahromi and Amir Mousavi conceived and designed the study, supervised the experiments, and contributed to the revision of the manuscript. Alireza Iranbakhsh contributed to data interpretation and assisted in the preparation of the manuscript. All authors reviewed, edited, and approved the final version of the manuscript for submission.

Compliance with Ethical Standards

Conflict of Interest The authors declare that they have no conflict of interest.

Data Availability Statement: All data generated or analyzed during this study are included in this published article. Raw data are available from the corresponding author upon reasonable request.

References

1. Ma L, Li J, Li J, Huo Y, Yang Y, Jiang C, Guo Y (2026) Plant salt-tolerance mechanisms: Classic signaling pathways, emerging frontiers, and future perspectives. *Mol Plant* 19(3):538-570. https://doi.org/10.1016/j.molp.2025.12.009
2. Kumar A, Singh R, Tiwari RK, Lal MK (2026) Effects of abiotic stress on the performance of horticultural crops. In: Altaf MA, Kumar R, Tiwari RK, Lal MK (eds) *Melatonin in Horticultural Plants*. Academic Press/Elsevier, pp 1-29. https://doi.org/10.1016/B978-0-443-33851-9.00009-9
3. Jahangiri E, Motamedvaziri B, Kiadaliri H (2025) Assessing the effect of climate change on drought and runoff using a machine learning model. *Int J Environ Sci Technol* 22(4):2205-2228. https://doi.org/10.1007/s13762-024-05917-w
4. Esmaeilzadeh Bahabadi S, Sharifi M, Behmanesh M, Ebrahimzadeh H (2020) Salinity stress alters ion homeostasis, antioxidant activities and the production of rosmarinic acid, luteolin and apigenin in *Dracocephalum kotschyi* Boiss. *Biologia* 75(12):2147-2158. https://doi.org/10.2478/s11756-020-00512-7
5. Rasheed A, Anwar S, Shafiq F, Khan S, Ashraf M (2024) Physiological and biochemical effects of biochar nanoparticles on spinach exposed to salinity and drought stresses. *Environ Sci Pollut Res* 31:14103-14122. https://doi.org/10.1007/s11356-024-32060-3
6. Seymen M, Yavuz D, Eroğlu S, Arı BÇ, Tanrıverdi ÖB, Atakul Z, Issı N (2023) Effects of different levels of water salinity on plant growth, biochemical content, and photosynthetic activity in cabbage seedling under water-deficit conditions. *Gesunde Pflanzen* 75:871-884. https://doi.org/10.1007/s10343-023-00953-x
7. Hassanpouraghdam MB, Abdollahfam F, Fathi S, Mehrabani LV (2023) Foliar application of iron-oxide nanoparticles coated with citral and chitosan enhances the growth and physiological responses of spearmint exposed to salinity stress. *Russ J Plant Physiol* 70:130. https://doi.org/10.1134/S1021443723601886
8. Junedi MA, Mukhopadhyay R, Manjari KS (2023) Alleviating salinity stress in crop plants using new engineered nanoparticles (ENPs). *Plant Stress* 7:100184. https://doi.org/10.1016/j.stress.2023.100184
9. Raza A, Tabassum J, Fakhar AZ, Sharif R, Chen H, Zhang C, Varshney RK (2023) Smart reprograming of plants against salinity stress using modern biotechnological tools. *Crit Rev Biotechnol* 43:1035-1062. https://doi.org/10.1080/07388551.2022.2093695
10. Adhikari B, Adhikari M, Ghimire B, Adhikari BC, Park G, Choi EH (2020) Cold plasma seed priming modulates growth, redox homeostasis and stress response by inducing reactive species in tomato (*Solanum lycopersicum*). *Free Radic Biol Med* 156:57-69. https://doi.org/10.1016/j.freeradbiomed.2020.06.003
11. Bian JY, Guo XY, Lee DH, Sun XR, Liu LS, Shao K, Liu K, Sun HN, Kwon T (2024) Non-thermal plasma enhances rice seed germination, seedling

development, and root growth under low-temperature stress. *Appl Biol Chem* 67(1):3. https://doi.org/10.1186/s13765-023-00856-9

12. Veerana M, Mumtaz S, Rana JN, Javed R, Panngom K, Ahmed B, Akter K, Choi EH (2024) Recent advances in non-thermal plasma for seed germination, plant growth, and secondary metabolite synthesis: a promising frontier for sustainable agriculture. *Plasma Chem Plasma Process* 44(6):2263-2302. https://doi.org/10.1007/s11090-024-10510-7
13. Abou El-Nasr MK, Hassan KM, Abd-Elhalim BT, Kucher DE (2025) The emerging roles of nanoparticles in managing the environmental stressors in horticulture crops—a review. *Plants* 14(14):2192. https://doi.org/10.3390/plants14142192
14. Zia-ur-Rehman M, Mfarrej MFB, Usman M, Anayatullah S, Rizwan M, Alharby HF, Ali S (2023) Effect of iron nanoparticles and conventional sources of Fe on growth, physiology and nutrient accumulation in wheat plants grown on normal and salt-affected soils. *J Hazard Mater* 458:131861. https://doi.org/10.1016/j.jhazmat.2023.131861
15. Singh A, Bol R, Lovynska V, Singh RK, Sousa JR, Ghazaryan K (2025) Application of nanoparticles for salinity stress management and biofortification in wheat: a review of dual approaches and insights. *Front Plant Sci* 16:1592866. https://doi.org/10.3389/fpls.2025.1592866
16. Landa P (2021) Positive effects of metallic nanoparticles on plants: Overview of involved mechanisms. *Plant Physiol Biochem* 161:12-24. https://doi.org/10.1016/j.plaphy.2021.01.040
17. Salehi H, Cheheregani Rad A, Raza A, Djalovic I, Prasad PV (2023) The comparative effects of manganese nanoparticles and their counterparts (bulk and ionic) in *Artemisia annua* plants via seed priming and foliar application. *Front Plant Sci* 13:1098772. https://doi.org/10.3389/fpls.2022.1098772
18. Kasote DM, Lee JH, Jayaprakasha GK, Patil BS (2021) Manganese oxide nanoparticles as safer seed priming agent to improve chlorophyll and antioxidant profiles in watermelon seedlings. *Nanomaterials* 11:1016. https://doi.org/10.3390/nano11041016
19. Rahman A, Nahar K, Hasanuzzaman M, Fujita M (2019) Manganese-induced salt stress tolerance in rice seedlings: regulation of ion homeostasis, antioxidant defense and glyoxalase systems. *Physiol Mol Biol Plants* 25(5):1215-1232. https://doi.org/10.1007/s12298-019-00697-z
20. Ye Y, Cota-Ruiz K, Hernández-Viezcas JA, Valdés C, Medina-Velo IA, et al. (2020) Manganese nanoparticles control salinity-modulated molecular responses in *Capsicum annuum* L. through priming: a sustainable approach for agriculture. *ACS Sustainable Chem Eng* 8(3):1427-1436. https://doi.org/10.1021/acssuschemeng.9b05615
21. Perfileva AI, Krutovsky KV (2024) Manganese nanoparticles: synthesis, mechanisms of influence on plant resistance to stress, and prospects for application in agricultural chemistry. *J Agric Food Chem* 72(14):7564-7585. https://doi.org/10.1021/acs.jafc.3c07350

22. Sun L, Wang Y, Wang J, Du Y, Li Y, Wu Z (2023) Manganese oxide nanoparticles alleviate salt-induced oxidative stress and promote root elongation in maize. *Environ Sci Nano* 10(2):456-469. https://doi.org/10.1039/D2EN00891C
23. Dixit N (2022) Salinity Induced Antioxidant Defense in Roots of Industrial Hemp (*Cannabis sativa* L.) for Fiber during Seed Germination. *Antioxidants* 11(2):244. https://doi.org/10.3390/antiox11020244
24. Hu H, Liu H, Liu F (2018) Seed germination of hemp (*Cannabis sativa* L.) cultivars responds differently to the stress of salt type and concentration. *Industrial Crops and Products* 123:254-261. https://doi.org/10.1016/j.indcrop.2018.06.089
25. Ghasempour S, Ghanbari Jahromi M, Mousavi A, Iranbakhsh A (2024) Seed priming with cold plasma, iron, and manganese nanoparticles modulates salinity stress in hemp (*Cannabis sativa* L.) by improving germination, growth, and biochemical attributes. *Environ Sci Pollut Res* 31:65315-65327. https://doi.org/10.1007/s11356-024-27094-1
26. Tzimas PS, Beteinakis S, Petrakis EA, Papastylianou PT, Kakabouki I, Small-Howard AL, Halabalaki M (2024) Uncovering the metabolite complexity and variability of cultivated hemp (*Cannabis sativa* L.): A first phytochemical diversity mapping in Greece. *Phytochemistry* 222:114076. https://doi.org/10.1016/j.phytochem.2024.114076
27. Formisano C, Fiorentino N, Di Mola I, Iaccarino N, Gargiulo E, Chianese G (2024) Effect of saline irrigation and plant-based biostimulant application on fiber hemp (*Cannabis sativa* L.) growth and phytocannabinoid composition. *Front Plant Sci* 15:1293184. https://doi.org/10.3389/fpls.2024.1293184
28. Wilson WB, Urbas AA, Abdur-Rahman M, Romares A, Mistek-Morabito E (2024) Determination of Δ9-THC, THCA, Δ8-THC, and total Δ9-THC in 53 smokable hemp plant products by liquid chromatography and photodiode array detection. *Forensic Chem* 37:100550. https://doi.org/10.1016/j.forc.2023.100550
29. Booth JK, Bohlmann J (2021) The biosynthesis of the cannabinoids. *J Cannabis Res* 3(1):7. https://doi.org/10.1186/s42238-021-00062-4
30. Ivankov A, Nauciene Z, Zukiene R, Degutyte-Fomins L, Malakauskiene A, Kraujalis P, Mildaziene V (2020) Changes in growth and production of non-psychotropic cannabinoids induced by pre-sowing treatment of hemp seeds with cold plasma, vacuum and electromagnetic field. *Appl Sci* 10:8519. https://doi.org/10.3390/app10238519
31. Iranbakhsh A, Oraghi Ardebili Z, Molaei H, Oraghi Ardebili N, Amini M (2020) Cold plasma up-regulated expressions of WRKY1 transcription factor and genes involved in biosynthesis of cannabinoids in hemp (*Cannabis sativa* L.). *Plasma Chem Plasma Process* 40:527-537. https://doi.org/10.1007/s11090-020-10067-1
32. Zulfiqar F, Nafees M, Chen J, Darras A, Ferrante A, Hancock JT, et al. (2022) Chemical priming enhances plant tolerance to salt stress. *Front Plant Sci* 13:946922. https://doi.org/10.3389/fpls.2022.946922

33. Savvides A, Ali S, Tester M, Fotopoulos V (2016) Chemical Priming of Plants Against Multiple Abiotic Stresses: Mission Possible? *Trends Plant Sci* 21(4):329-340. https://doi.org/10.1016/j.tplants.2015.11.003
34. Xi J, Wang Y, Zhou X, Wei S, Zhang D (2024) Cold plasma pretreatment technology for enhancing the extraction of bioactive ingredients from plant materials: A review. *Ind Crop Prod* 209:117963. https://doi.org/10.1016/j.indcrop.2024.117963
35. Mardani Korrani H, Iranbakhsh A, Ebadi M, Oraghi Ardebili Z (2024) RBOH-dependent signaling is involved in He-Ne laser-induced salt tolerance and production of rosmarinic acid and carnosol in *Salvia officinalis*. *BMC Plant Biol* 24:798. https://doi.org/10.1186/s12870-024-05502-w
36. Yang et al. (2024) *[Please add full citation – missing from your original list]*
37. Ghasemzadeh N, Iranbakhsh A, Oraghi-Ardebili Z, Saadatmand S, Jahanbakhsh-Godehkahriz S (2022) Cold plasma can alleviate cadmium stress by optimizing growth and yield of wheat (*Triticum aestivum* L.) through changes in physio-biochemical properties and fatty acid profile. *Environ Sci Pollut Res* 29:35897-35907. https://doi.org/10.1007/s11356-022-18610-7
38. Roosta HR, Estaji A, Khadivi A, Shams M (2025) Balanced ammonium–nitrate nutrition enhances photosynthetic efficiency, micronutrient homeostasis, and antioxidant networks via ROS signaling in *Glycyrrhiza glabra* across soil and soilless systems. *Sci Rep* 15(1):25404. https://doi.org/10.1038/s41598-025-11181-w
39. Shams M, Pokora W, Khadivi A, Aksmann A (2024) Superoxide dismutase in *Arabidopsis* and *Chlamydomonas*: diversity, localization, regulation, and role. *Plant Soil* 503(1):751-771. https://doi.org/10.1007/s11104-024-06618-6
40. Hädener M, König S, Weinmann W (2019) Quantitative determination of CBD and THC and their acid precursors in confiscated cannabis samples by HPLC-DAD. *Forensic Sci Int* 299:142-150. https://doi.org/10.1016/j.forsciint.2019.03.044
41. Brands M, Gutbrod P, Dörmann P (2021) Lipid analysis by gas chromatography and gas chromatography–mass spectrometry. In: *Plant Lipids: Methods and Protocols*, Springer US, pp 43-57. https://doi.org/10.1007/978-1-0716-1362-7_4
42. Shirkhani Z, Hassanabadi Z, Abomughid MM, Ahmed HH, Hamid HK (2025) Cold Plasma enhances melatonin and brassinosteroids efficacy by regulating physio-biochemical characteristics in summer savory (*Satureja hortensis* L.) exposed to soil chromium toxicity. *J Soil Sci Plant Nutr* 24:1-16. https://doi.org/10.1007/s42729-024-01688-w
43. Sayahi K, Sari AH, Hamidi A, Nowruzi B, Hassani F (2024) Evaluating the impact of Cold plasma on Seedling Growth properties, seed germination, and soybean antioxidant enzyme activity. *BMC Biotechnol* 24:93. https://doi.org/10.1186/s12896-024-00872-3

44. Liu K, Feng YJ, Guo JX, Wang GL, Shan LL, Gao SW, Kwon T (2024) Argon non-thermal plasma treatment promotes the development of rice (*Oryza sativa* L.) in saline alkali environments. *Protoplasma* 261:927-936. https://doi.org/10.1007/s00709-024-01928-z
45. He M, Ding NZ (2020) Plant unsaturated fatty acids: multiple roles in stress response. *Front Plant Sci* 11:562785. https://doi.org/10.3389/fpls.2020.562785
46. Abdi MJ, Ghanbari Jahromi M, Mortazavi SN, Kalateh Jari S, Nazarideljou MJ (2023) Foliar-applied silicon and selenium nanoparticles modulated salinity stress through modifying yield, biochemical attribute, and fatty acid profile of *Physalis alkekengi* L. *Environ Sci Pollut Res* 30:100513-100525. https://doi.org/10.1007/s11356-023-29476-8
47. Amirfakhrian Z, Abdossi V, Mohammadi Torkashvand A, Weisany W, Ghanbari Jahromi M (2024) Co-applied magnesium nanoparticles and biochar modulate salinity stress via regulating yield, biochemical attribute, and fatty acid profile of *Physalis alkekengi* L. *Environ Sci Pollut Res* 31:31806-31817. https://doi.org/10.1007/s11356-024-33406-7
48. Amooaghaie R, Tabatabaei S, Ahadi AM (2017) Impact of zinc and zinc oxide nanoparticles on the physiological and biochemical processes in tomato and wheat. *Botany* 95(6):529-539. https://doi.org/10.1139/cjb-2016-0194
49. Amooaghaie R, Mardani Korrani F, Ghanadian M, Ahadi A, Pak A, Mardani G (2024) Hybrid Priming with He–Ne Laser and Hydrogen Peroxide Advances Phenolic Composition and Antioxidant Quality of *Salvia officinalis* Under Saline and Non-Saline Condition. *J Plant Growth Regul* 43(4):1012-1025. https://doi.org/10.1007/s00344-023-11156-z

a

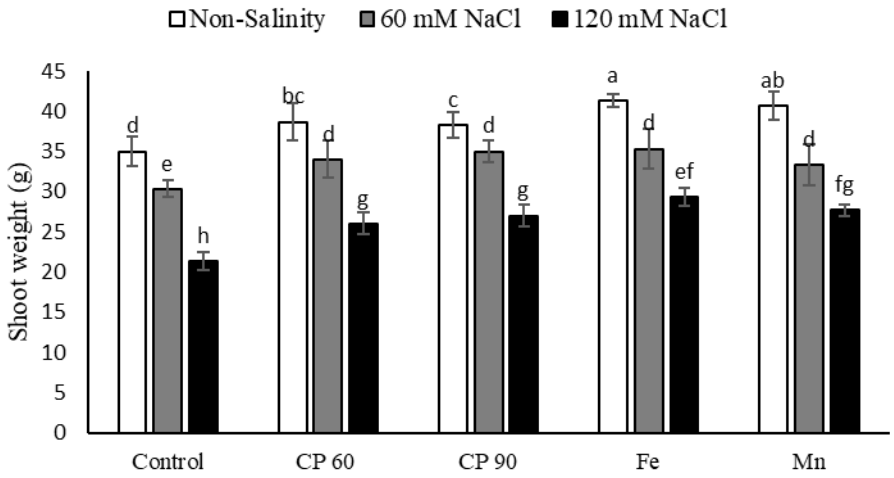

b

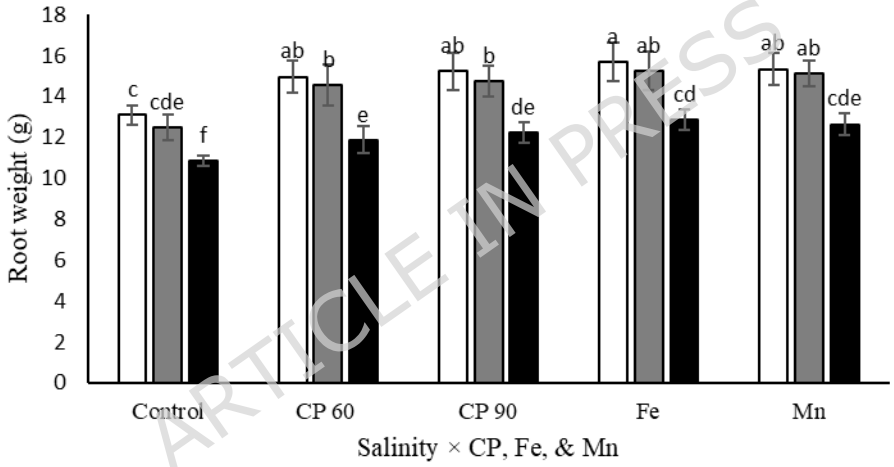

Fig. 1. Biomass partitioning in hemp as affected by salinity stress and seed priming treatments (cold plasma (CP 60s, CP 90s), Fe NPs, Mn NPs): (a) shoot fresh weight and (b) root fresh weight. Different letters denote statistically significant differences ($p \leq 0.05$). Error bars represent ± SE.

a

Fig. 2.

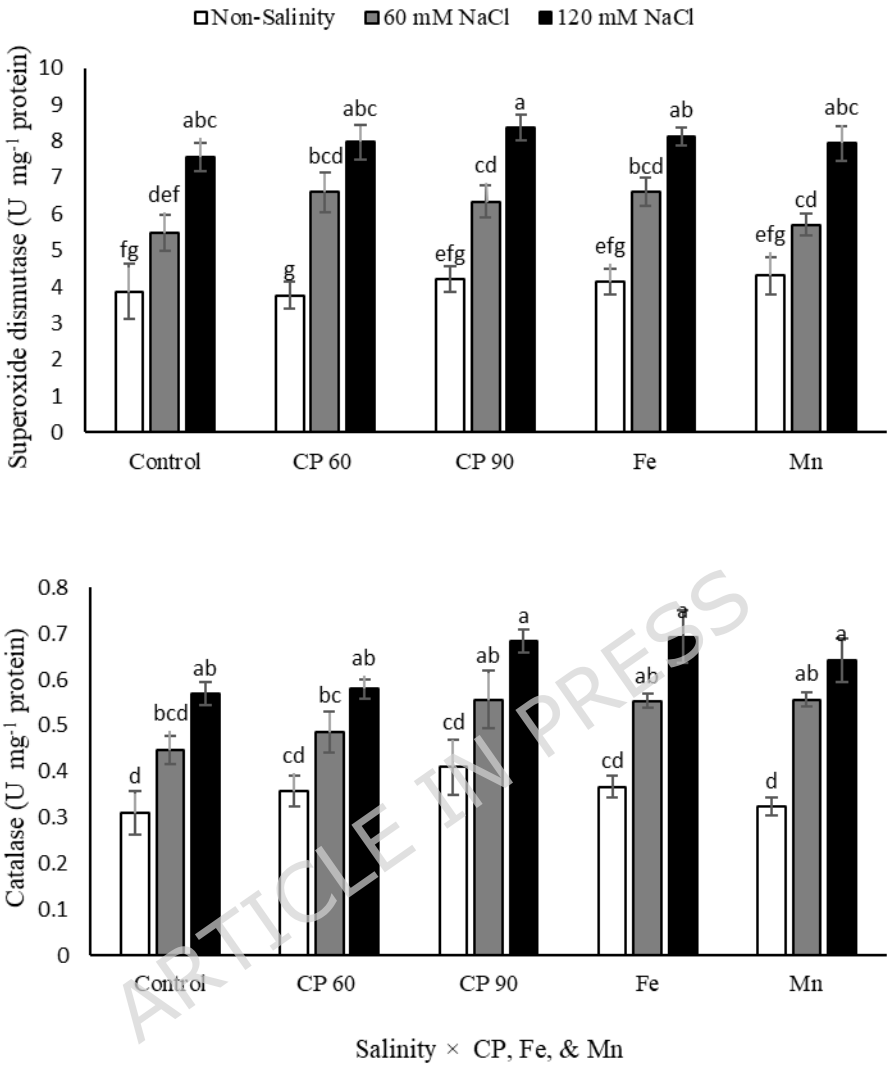

Superoxide dismutase (a) and catalase (b) activities of hemp plants under salinity and seed priming with cold plasma (CP), iron (Fe) and manganese (Mn) nanoparticles. Letters above the column represents the statistical significance and bars are standard error.

Fig a ditions: (a) car entrations. Sta tters. Data are

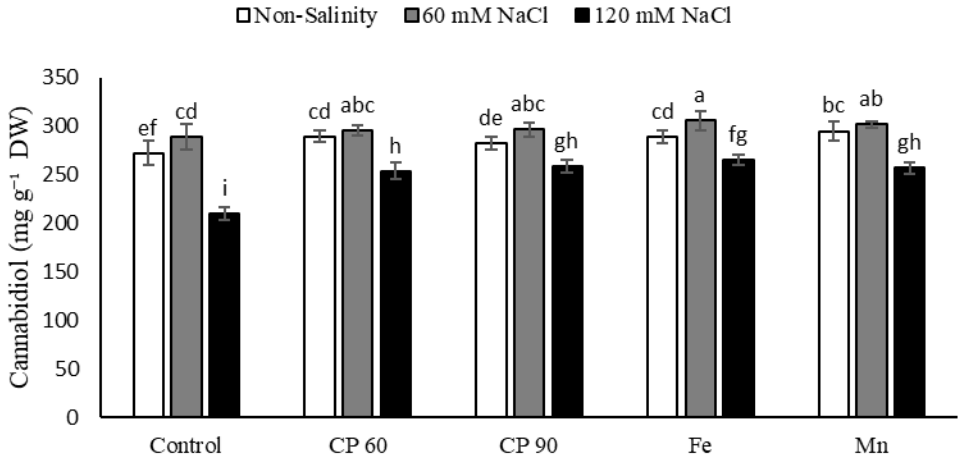

a

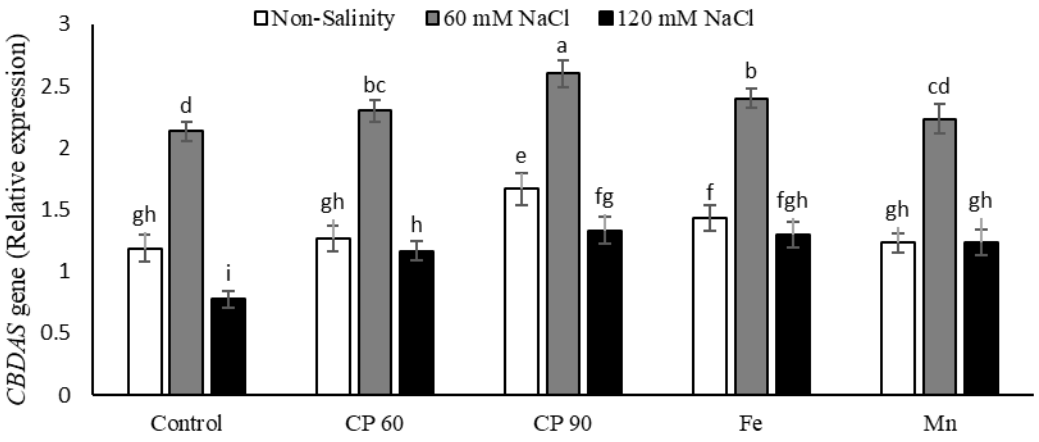

b

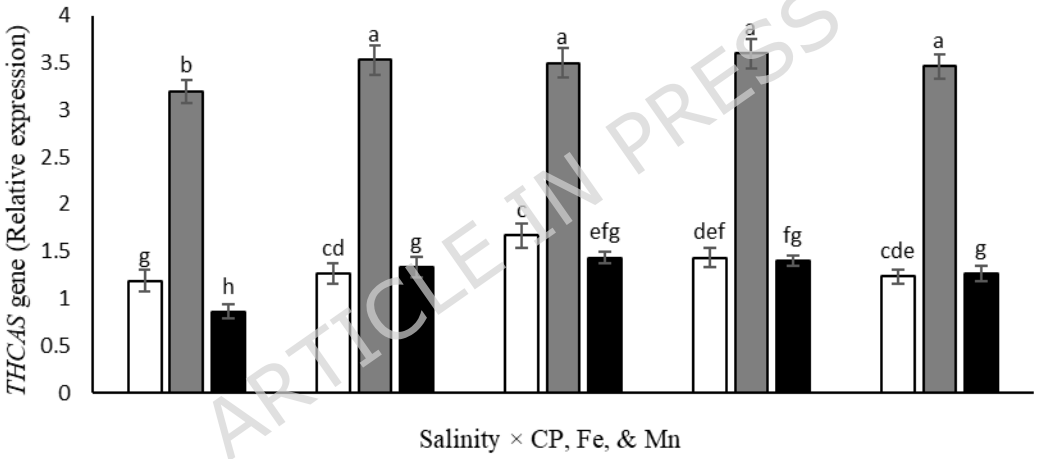

Fig. 4.

and (b)
SD, $p \leq$

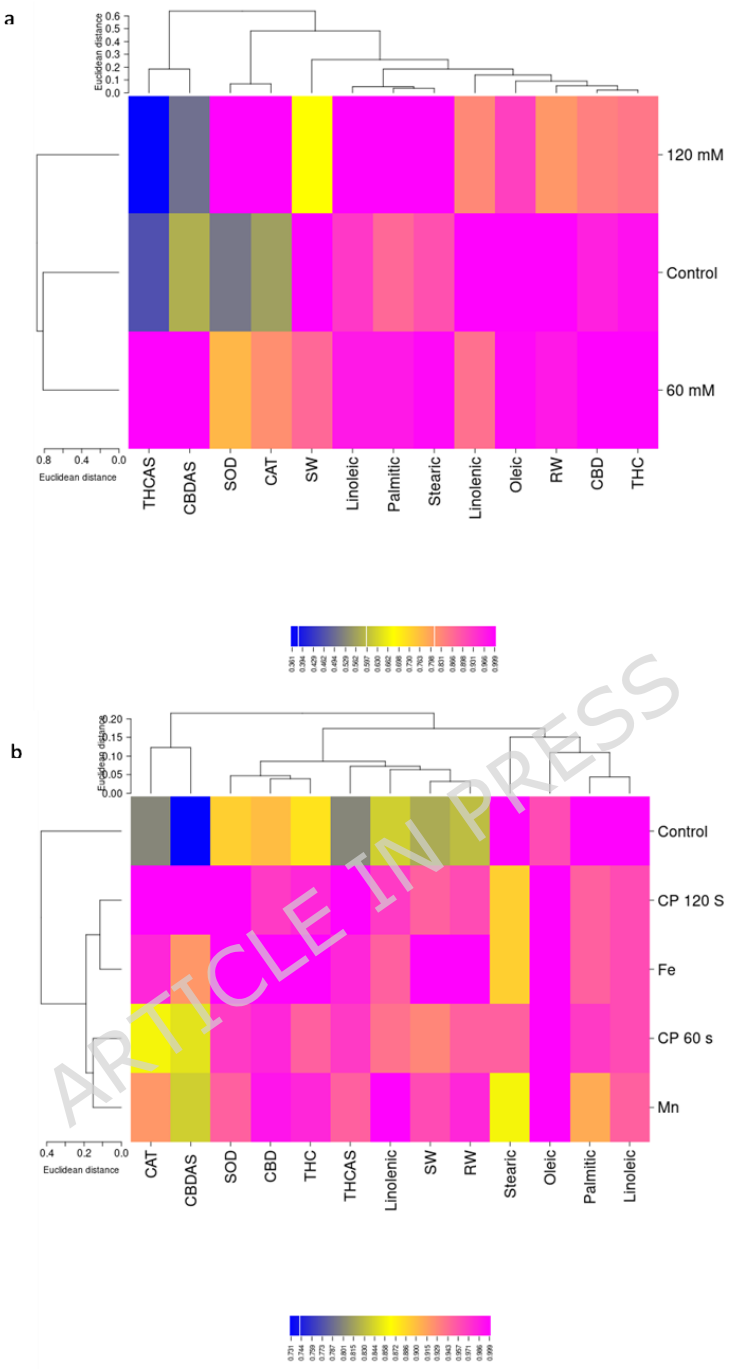

Fig. 5. Hierarchical clustering analysis visualized by heat map for (a) salinity levels and (b) seed priming treatments. Abbreviations: CBD, cannabidiol; THC, tetrahydrocannabinol; SW, shoot weight; RW, root weight; Chl, chlorophyll; RWC, relative water content; TPC, total phenolic content; TFC, total flavonoid content.

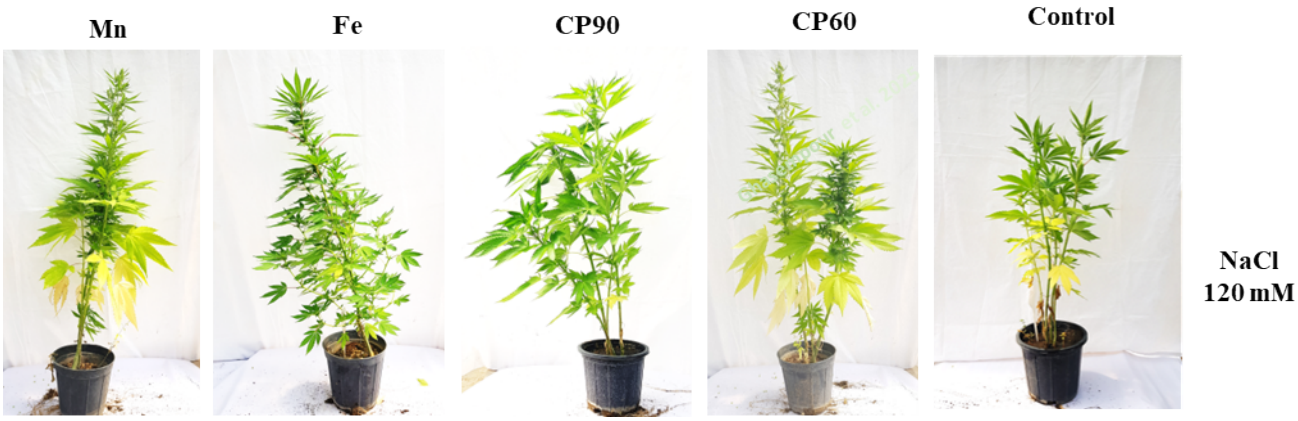

Fig. 6 Appearance of hemp plants under salinity (NaCl 120 mM) and seed priming with cold plasma (CP), iron (Fe) and manganese (Mn) nanoparticles.

Table 1. Primers sequences and characteristics utilized for this study

Locus	Sequence	Amplicon length (bp)	Accession
THCAS-F	GATCAGCTGGGAAGAAGACG	188	XM_061118802.1
THCAS-R	ATGAGGGAATGGAATTGCTG		
CBDAS-F	CTCTTCCACGGCATCGTCAT	123	NM_001397936.1
CBDAS-R	GCATACACAGTACATCCGGACA		
UBQ-F	ACCAATCCAGATGTTCCACCTG	100	XM_030630092.2
UBQ-R	GCAATGCCCTGATGTTCTCTTG		

Table 2. Modulation of the fatty acid composition in hemp seeds under salinity stress and seed priming treatments (cold plasma, Fe NPs, Mn NPs)

Salinity	Priming	Palmitic acid	Stearic acid	Oleic acid	Linoleic acid	Linolenic acid
Non-salinity	Control	5.97±0.34^{bcde}	2.43±0.03^{ab}	18.57±0.51^{a}	54.67±0.78^{bcd}	18.37±0.81^{bcd}
	CP 60 s	5.93±0.16^{bcde}	2.23±0.21^{b}	18.7±0.32^{a}	52.67±1.06^{cde}	20.47±1.05^{abc}
	CP 90 s	5.8±0.2^{cde}	2.33±0.11^{ab}	18.3±0.59^{ab}	52.33±1.56^{de}	21.23±0.79^{ab}
	Fe NPs	5.6±0.35^{e}	2.37±0.13^{ab}	18.6±0.32^{a}	53.33±1.06^{bcde}	20.1±0.79^{abc}
	Mn NPs	5.37±0.19^{e}	2.23±0.21^{b}	18.87±0.43^{a}	51.33±0.78^{e}	22.2±0.47^{a}
60 mM NaCl	Control	6.7±0.39^{ab}	2.87±0.18^{a}	17.7±0.65^{ab}	56.67±0.29^{ab}	16.07±1.31^{de}
	CP 60 s	6.27±0.23^{abcd}	2.77±0.16^{ab}	18.6±0.42^{a}	54±0.51^{bcde}	18.37±0.82^{bcd}
	CP 90 s	6.43±0.33^{abcd}	2.33±0.11^{ab}	18.8±0.31^{a}	54.67±0.29^{bcd}	17.77±0.67^{cde}
	Fe NPs	6.6±0.36^{abc}	2.4±0.14^{ab}	18.43±0.16^{ab}	55±0.51^{bcd}	17.57±0.7^{cde}
	Mn NPs	5.8±0.23^{cde}	2.33±0.11^{ab}	18.77±0.33^{a}	55±0.51^{bcd}	18.1±0.6^{bcd}
120 mM NaCl	Control	6.87±0.31^{a}	2.8±0.14^{ab}	16.13±0.46^{c}	59.33±1.79^{a}	14.87±1.34^{e}
	CP 60 s	6.7±0.26ab	2.67±0.21^{ab}	17.47±0.45^{ab}	56.67±0.59^{ab}	16.5±1.11d^{e}

CP 90 s	6.33±0.26^{abcd}	2.53±0.13^{ab}	17.57±0.41^{ab}	56±1.02^{bc}	17.57±0.24^{cde}
Fe NPs	6.3±0.22^{abcd}	2.43±0.16^{ab}	17.77±0.36^{ab}	55.33±0.59^{bcd}	18.17±0.74^{bcd}
Mn NPs	6.57±0.38^{abc}	2.43±0.12^{ab}	17.07±0.62^{bc}	55.67±1.06^{bcd}	18.27±0.42^{bcd}

Superscripted letters represent the statistical significance and bars are standard error. CP: cold plasma; Mn NPs: manganese nanoparticles; Fe NPs: iron nanoparticles.